NUCET NUCLEAR ENERGY AND TECHNOLOGY

Nuclear Energy and Technology 5(1): 23–29
DOI 10.3897/nucet.5.33978

Research Article

Peculiarities of the radiation formation in dispersed microencapsulated nuclear fuel*

Sergey V. Bedenko[1], Vladimir V. Knyshev[1], Mariya Ye. Kuznetsova[1], Igor O. Lutsik[1], Igor V. Shamanin[1]

1 *National Research Tomsk Polytechnic University, 2 prospekt Lenina, Tomsk, 634050, Russia*

Corresponding author: *Sergey V. Bedenko* (bedenko@tpu.ru)

Academic editor: *Yury Kazansky* ♦ **Received** 12 June 2018 ♦ **Accepted** 2 October 2019 ♦ **Published** 20 March 2019

Citation: Bedenko SV, Knyshev VV, Kuznetsova MY, Lutsik IO, Shamanin IV (2019) Peculiarities of the radiation formation in dispersed microencapsulated nuclear fuel. Nuclear Energy and Technology 5(1): 23–29. https://doi.org/10.3897/nucet.5.33978

Abstract

A computational study has been performed for various options of the thorium reactor core loading. Neutronic studies of fuel have been conducted, its isotopic composition has been calculated, and the alpha emitters and the sources of neutron and photon radiation in the microencapsulated nuclear fuel have been analyzed. The studies had the purpose of developing the methodology used to estimate the radiation characteristics of nuclear fuel with a complex inner structure. Emphasis is placed on calculating the quantitative and spectral composition of the neutrons formed as the result of (α, n) reactions on small- and average-mass nuclei. The ratio of the quantity of the neutrons resulting from the (α, n) reactions to the quantity of the neutrons formed as the result of spontaneous fission has been calculated for fuel with heterogeneous and homogeneous arrangements of fissionable and structural elements. The developed tools will make it possible to estimate the neutron radiation dose, to revise the traditional fresh and spent fuel handling procedures, and to estimate, using the Rossi alpha method, the neutron multiplication factor in deeply subcritical systems. The neutron yield and spectrum were calculated using an analytical model and verified codes such as WIMS-D5B, ORIGEN-APP, SOURCES-4C and SRIM-2013.

Keywords

Thorium reactor; isotopic composition; alpha particle transport; neutron source; spectrum of radiation sources

Introduction

In (Shamanin et al. 2015, Shamanin et al. 2016, Shamanin et al. 2018), the author studied the physics of a small high-temperature gas-cooled thorium reactor plant (HGTRU, Russia), and selected the best reactor core configuration and the best nuclear fuel material composition. The reactor considered in (Shamanin et al. 2018) is capable to operate for not less than 3000 effective days at a power level of 60 MW. Peculiarities of the reactor core design, the material composition of dispersed microencapsulated nuclear fuel (microfuel), and operating conditions affect the radiation characteristics of fuel and require traditional nuclear fuel handling procedures to be revised at the reactor design stage.

Emphasis in the study is placed on calculating the neutron component of the dispersed nuclear fuel's radiation characteristics. Neutrons are formed in nuclear fuel due to spontaneous and induced fissions, and as a result of (α, n) reactions on small- and average-mass nuclei (Vlaskin et al.

* Russian text published: Izvestiya vuzov. Yadernaya Energetika (ISSN 0204-3327), 2018, n. 3, pp. 75–87.

2015, Bulanenko 1979, Murata and Shibata 2002, West and Sherwood 1982). In such studies, the yield q_{sf} and the spectral distribution (spectrum) of spontaneous fission neutrons $S_{sf}(E)$ are comparatively easy to determine. For this reason, of greater interest is determination of the ratio of the quantity of the neutrons $q_{\alpha n}$ formed as a result of (α, n) reactions to the quantity of the neutrons resulting from spontaneous (q_{sf}) and induced (q_f) fission (in the event of large-size spent nuclear fuel (SNF) blocks) which is of interest both for calculating the neutron radiation dose rate during handling of such fuel (Dulin and Zabrodskaya 2005, Dulin and Matveyenko 2002) and in using the Rossi alpha method to determine the multiplication factor (k_{eff}) in subcritical systems (Dulin and Matveyenko 2002), such as the HGTRU fuel block (Shamanin et al. 2018). This problem was examined rather thoroughly and solved in (Vlaskin et al. 2015, Bulanenko 1979, Dulin and Zabrodskaya 2005, Dulin and Matveyenko 2002, Shamanin et al. 2017, Bogatov et al. 2015) and as part of other studies for fuel in the form of homogeneous dioxide. In the event when dispersed fuel and media containing heterogeneous inclusions of different configurations and sizes are considered, this problem is more difficult to solve and the method to calculate the quantitative and spectral compositions of the neutron source is of interest as such.

The purpose of the study is to develop the methodology to calculate the quantitative and spectral compositions of the neutron radiation source with a heterogeneous arrangement of fissionable and structural elements in nuclear fuel. Such studies are conducted with the use of verified codes and dedicated programs. It often turns out during numerical modeling of radiation fields and in development of new procedures and regulations for the SNF handling in a nuclear fuel cycle of a new generation (Shamanin et al. 2018, Bogatov et al. 2015, Glukhov et al. 2016, Spirin et al. 2015) that no standard codes can be used without respective scientific rationale and upgrades. For instance, the ORIGEN-S code enables determination of the nuclear fuel nuclide composition and the spectral composition of the SNF neutron and photon radiation sources depending on burn-up and decay time. This code is one of the advanced tools used internationally to calculate radiation sources. It is normally employed to calculate the burn-up and radiation sources of standard oxide fuel (UO_2, $(U,Pu)O_2$) for LWR-type reactors, while the use of ORIGEN-S may lead to incorrect results in the event of other reactor types and for fuel other than of the standard type (Bogatov et al. 2015). It should be noted that, apart from ORIGEN-S, there are other neutron source codes, e.g., SOURCES-4C (Wilson et al. 2009), NEDIS-2m (Vlaskin and Khomyakov 2017), CHARS (Leniau and Wilson 2014), and others (Spirin et al. 2015, Vlaskin and Khomyakov 2017). These codes fully focus on the neutron yield and spectrum calculation; the most commonly used code is SOURCES-4C, as the NEDIS-2m code (Vlaskin et al. 2015, Spirin et al. 2015, Vlaskin and Khomyakov 2017) is the one best adapted to problems of present-day nuclear power.

The nuclear reactor considered in (Shamanin et al. 2018) is a reactor plant using prompt neutrons (~63.03 % of neutrons with an energy of 4 eV to 183 keV) and fast neutrons (~24.5 % of neutrons with an energy of 183 keV to 10 MeV) with the $(Th,Pu)O_2$ composition used as nuclear fuel. The (α, n) reaction can run in the nuclear fuel of such reactor not only on $^{17,18}O$ isotopes but also on ^{13}C and $^{29,30}Si$ contained in the microfuel (Ti_3SiC_2) and fuel pellet (SiC) coatings. The rated neutron spectrum $\chi_{\alpha n}(E)$ on ^{13}C and $^{29,30}Si$ is much higher than the (α, n) neutron spectrum on $^{17,18}O$ (Bulanenko 1979, Jacobs and Liskien 1983), and the content of ^{13}C carbon in the pellet matrix may reach 62.5 %.

For unirradiated dispersed nuclear fuel, $\chi_{\alpha n}(E)$ and $S_{\alpha n}(E)$ can be calculated using available high-accuracy experimental data (Experimental Nuclear Reaction Data, see https://www-nds.iaea.org/exfor/exfor.htm) and special-purpose codes (NEDIS-2.0, SOURCES-4C, SRIM-2013 (Ziegler et al. 2010)). To obtain the correct result, though, it is enough to take into account the energy distribution of alpha particles $f_\alpha(E)$ within the fuel kernel and in the coatings (Bedenko et al. 2018). The distribution $f_\alpha(E)$ can be obtained provided the sources of alpha particles (^{232}Th,$^{239,240,241}Pu$) are distributed uniformly within the kernel and create spherically symmetrical radiation.

The irradiated fuel kernel represents a mixture of unburnt Pu and Th isotopes, minor actinides, oxygen, and fission fragments. The initial functions $f_\alpha(E)$, $\chi_{\alpha n}(E)$ and $S_{\alpha n}(E)$ in such kernel will depend on the distribution $P(E, r)$ of heavy isotopes and fission fragments within it, which complicates considerably the conditions of the problem, as the use of (Fomushkin 2010, Bak et al. 1965) and other similar models requires a scientific rationale.

Investigation techniques and approximations

The energy distribution of neutrons $\chi_{\alpha n}(E)$, $S_{\alpha n}(E)$ sought after depends in a general case on the geometry of the fuel pellet and the material composition of nuclear fuel, the reactor type and operating modes, and the distribution of radiation sources (Pu, Th, minor actinides) $f_{HM}(r)$, fission products $f_{FP}(r)$, and alpha particles $f_\alpha(E, r)$ within the fuel kernel, on the fuel surface and in the coatings.

Three types of fuel pellets designated 0817, 1017 and 1200 were used in (Shamanin et al. 2018); the authors have shown that an increase in the fuel pellet diameter leads to a smaller fraction of graphite and a reduced reactivity margin $\rho_{inf}(t)$, and the reactor life depends on the initial quantity of ^{239}Pu and ^{232}Th and on the quantity of the ^{241}Pu and ^{233}U formed. When a fuel pellet of the type 0817 is used, ^{239}Pu burns out rapidly and ^{233}U and ^{241}Pu do not have enough time to accumulate in such quantity as required for maintaining the steady-state fission reaction. Therefore, after 1500 days of operation, the quantity of ^{239}Pu and ^{239}Pu left in the reactor is too small and $\rho_{inf}(t)$

decreases abruptly. The use of pellets of the types 1017 and 1200 leads to the accumulation of ^{233}U and ^{241}Pu and to longer operation of the reactor. We shall note that the burn-up of ^{239}Pu is practically the same for the pellets of the types 0817 and 1017 amounting to 96 and 97% respectively. Therefore, the option with a fuel pellet of the type 1200 is the best one in terms of lifetime and the involvement of ^{232}Th in the fuel cycle, but an increase in the dispersed phase fraction in such pellet (ω_{fuel}) will lead to a smaller fraction of the burnt-out ^{239}Pu. The analysis of results in (Shamanin et al. 2015, Shamanin et al. 2016, Shamanin et al. 2018) shows that the best burn-up of ^{239}Pu requires the selection of a fuel pellet of the type 1017 (Fig. 1).

Further neutronic experiments were conducted in WIMS-D5B, a versatile code for calculating the cell of different reactor types. The WIMS code uses a 69-group system of constants based on the evaluated nuclear database, ENDF/B-VII.0, which makes it possible to calculate fast and thermal neutron reactors.

The geometry module of the WIMS code is not capable to create cells of a hexagonal shape, so the hexagonal HGTRU cell (Shamanin et al. 2018) was transformed into a 2D cylindrical cell. The cylindrical cell is an equivalent Wigner-Seitz cell with preset boundary conditions on the calculated area surface and with a translational symmetry on the upper and lower faces. To calculate k_{eff}, axial and radial geometrical parameters are introduced as calculated with regard for the transition from the actual core size to the equivalent Wigner-Seitz system (see Fig. 1b).

Computational studies were performed for 30 reactor core loading options differing in composition. The content of heavy metal in the pellet kernels (%) for all of the calculated options is as follows: Pu – 50, ^{232}Th – 50. The isotopic composition of Pu (%): 238 – 0, 239 – 94, 240 – 5.4; 241 – 0.6; 242 – 0. The results of the studies are shown in Fig. 2 where it can be seen that an over 17-18% increase of ω_{fuel} is not reasonable since the fuel life increases insignificantly, and the share of the burnt-out ^{239}Pu will decrease.

We shall note that the overall nature of the dependence $t(\omega_{fuel})$ (see Fig. 2) obtained for the full-scale heterogeneous reactor model will be the same. The results ω_{fuel} and t will be not differ significantly, despite the fact that the homogenization of the cell's fuel portion leads to a 3 to 7% reduction of k_{eff} in relation to more accurate modeling (Chukbar 2015).

Thus, we have selected a fuel pellet of the type 1017 with the dispersed phase content of 17 % (see Fig. 2). For a fuel pellet of the type 1017 with ω_{fuel} = 17 % and the reactor thermal power of P = 60 MW, the reactor life will be ~3000 days (see Fig. 2). In a cell of such reactor, ^{239}Pu burns up to 84.5%, ^{240}Pu to 36.9%, and ^{232}Th to 9.68%.

Irradiated microfuel represents a complex mixture of isotopes, so the functions $f_{\alpha}(E)$, $\chi_{\alpha n}(E)$ and $S_{\alpha n}(E)$ sought after will depend on the density distribution of the probability of interactions $P(E, r)$ for the considered radiation within the kernel. The density of the probability of neutron interactions

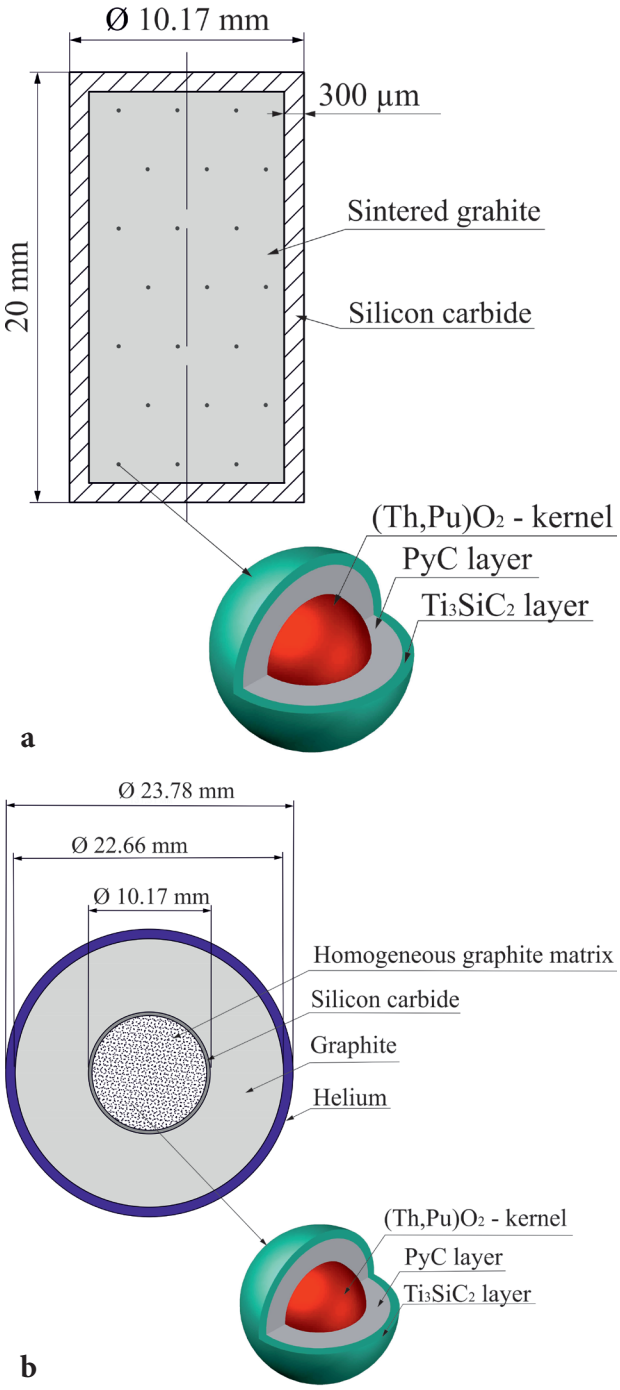

Figure 1. Fuel pellet of the type 1017 (a) and a 2D computational model of the equivalent cell (b).

$P(l_0, r)$ within the kernel at the distance r from its center (Fomushkin 2010) can be described by the function of the form

$$P(l_0, r) = \int v(x, r) \times \Psi(x) dx, \quad (1)$$

where $v(x, r)$·is the probability for experiencing the interaction within the kernel at the distance r from its center; $\Psi(x)$ is the exponential law of the neutron radiation attenuation in the kernel material; $l_0 = \lambda_t / R$ is the rated neutron path length; λ_t is the average-weighted neutron path; and R is the kernel radius.

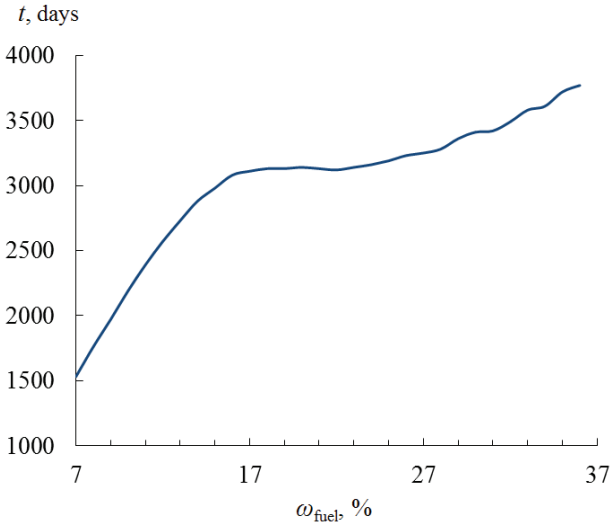

Figure 2. Duration of operation as a function of fraction of dispersed phase.

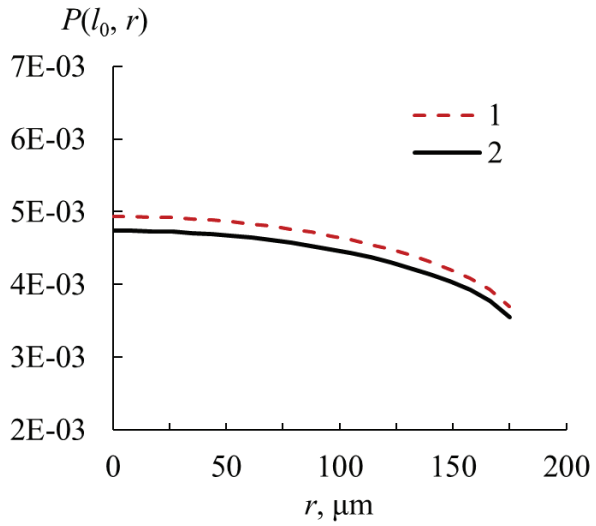

Figure 3. Probability density of the neutron interactions within the kernel: 1 – l_{01} = 91; 2 – l_{02} = 93.

As of the time of the irradiation start, $\lambda_{t1} = 1/\Sigma_{t1} = 1/0.309 = 3.24$ cm, $l_{01} = 93$, and $\lambda_{t2} = 1/0.313 = 3.19$ cm, $l_{02} = 91$ as of the irradiation cycle end. The average-weighted value of the neutron free path λ_t calculated with regard for the spectrum of the neutron flux $\varphi_n(E)$ (Shamanin et al. 2018) was used to estimate l_0, that is, all materials of the fuel pellet (graphite matrix, kernel and coatings) can see one and the same spectrum. The diagram of the dependence of $P(l_0, r)$ for several values of l_0 is presented in Fig. 3. It can be seen (Fig. 3) that the distribution of $P(l_0, r)$ for $l_{01 \text{ and }} l_{02}$ ($\lambda_t >> R$) is practically uniform ($P(l_{01.02}, 0)/P(l_{01.02}, 175) = 1.26$) and differs greatly from $P(l_{04}, r)$ for the case when $\lambda_t \approx R$ (Fomushkin 2010). We shall note that, with $\lambda_t << R$, the probability $P(l_{03,04,} r)$ is greater in the kernel's peripheral portion (Fomushkin 2010), that is, the fragments formed from fission will shield the inner part of the kernel from the incident neutron flux. The "grain self-shielding" effect is taken into account practically by all neutron transport codes. Model (Fomushkin 2010) makes it possible to estimate the grain self-shielding effect ($\lambda_t < R$), so will give consequently a correct result for the case when the neutron free path length is much greater than the kernel's cross-section dimension ($\lambda_t >> 2R$).

We shall assume that heavy isotopes in the kernel burn out uniformly ($P(l_0, r) = 1.26 \approx 1$), so, then, the sources of alpha particles and fission fragments are distributed uniformly and homogeneously within the kernel as of the end of irradiation and the spatial distribution $f_{FP}(r)$ of fission fragments, as shown in (Fomushkin 2010), can be determined from the relation

$$f_F(l,r) = \begin{cases} 3/4\pi, & 0 \le l \le 1-r; \\ \dfrac{3}{4\pi}\left(1/2 - l/4r + (1-r^2)/4rl\right), & 1-r \le l \le 1+r; \\ 0, & l \le 1-r. \end{cases}$$

where $r = x/R$; $l = \lambda/R$; and λ is the fission fragment path in the kernel.

The average energy of excitation for a light-weight fragment ($A_1 = 90$) is equal to about 10 MeV, and that of a heavy-weight fragment ($A_2 = 140$) is equal to about 8 MeV. The path length of light-weight fragments in the kernel material as of the end of irradiation will be 4 to 7 μm ($l_1 = \lambda/R$ = 4 μm / 175 μm = 0.023), and their spatial distribution (Fig. 4, line 1), similarly to the case of heavy metals (except the peripheral layer), does not depend on r.

The computational studies performed have helped to formulate the following assumptions.

1. The irradiated kernel is a homogeneous mixture of heavy isotopes, fission fragments, and oxygen.
2. The sources of alpha particles, alpha particles as such and fission fragments are distributed uniformly and homogeneously in the kernel.
3. Each source creates isotropic and spherically symmetrical radiation.
4. The functions $\chi_{\alpha n}(E)$ and $S_{\alpha n}(E)$ depend only on the differential energy spectrum of alpha particles $f_\alpha(E) = dN_\alpha(E)/dE$ inside of the kernel and on its surface.

Intensity and energy spectrum of alpha particles

The subject of the study is the HGTRU microfuel and fuel pellet. The configuration of the kernel, the coatings and the fuel pellet is shown in Fig. 1. To find $f_\alpha(E)$, one needs to solve the problem of the kernel surface radiation. A similar problem was solved, e.g., in (Fomushkin 2010, Bak et al. 1965) and by other researchers, and the theoretical basis can be found in training books on theory of grids.

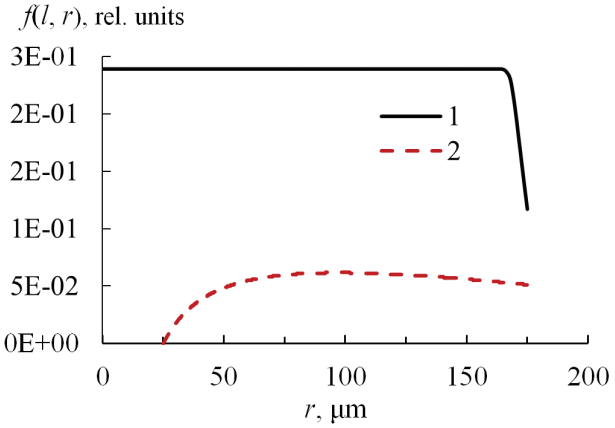

Figure 4. Spatial distribution of fission fragments within the kernel: 1 – l_1 = 0.023; 2 – l_2 = 1.

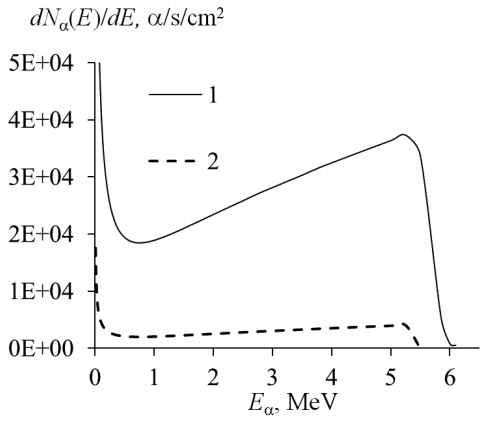

Figure 5. Spectrum of alpha particles escaping from the kernel surface at a solid angle of 4p (1 – irradiated fuel; 2 – unirradiated fuel).

The fraction of the radiation P (probability) from the inside of the kernel in (Bak et al. 1965) was obtained for a source with self-absorption:

$$P = \frac{3}{4(\mu R)^3}\left((\mu R)^2 - 0.5 + (\mu R + 0.5)\exp(-2\mu R)\right), \quad (2)$$

where $\mu = 1/\lambda_0$ is the absorption coefficient; and λ_0 is the average particle path.

Relation (2) is valid with any μR, but $f(x)dx = \exp(-x/\lambda_0)dx/\lambda_0$ for the particles (neutrons, gamma-quanta) the path of which is described by an exponential distribution. In the event of $\mu R >> 1$ ($\lambda_0 << R$), the key role in (2) is played by the first term and then $P \approx 3\lambda_0/(4R)$. The probability P sought after in (Bak et al. 1965) was obtained as a triple integral, the subintegral function was expanded into series, and a term-wise integration was performed, after which the infinite series was summed up. All these operations are quite cumbersome for a general problem but they are simplified to a great extent with $\lambda_0 << R$, as the obtained solution is valid also for particles with a fixed free path (alpha particles, fission fragments, protons). In (Fomushkin 2010), the solution to this problem was obtained thanks to using principles of geometrical probabilities. Such approach makes it possible to reduce the finding of a general solution to elementary computations of volumes and to the subsequent integration of fairly simple functions. In (Fomushkin 2010), the author considered different types of radiation, including radiation with a fixed free path. For radiation with a fixed and relatively short path of ($\lambda \le R$), the probability P is given by the formula

$$P = 0.75\lambda R^{-1} - 0.0625(\lambda/R)^3, \quad \lambda << R, \quad P \approx 3\lambda/(4R).$$

If the full number of the alpha particles formed in the kernel at the time of the decay is equal to $N_{\alpha 0}$, and $P_\alpha(E)$ is the fraction of the radiation escaping from the kernel, then the number of the alpha particles remaining in and those leaving the kernel is equal respectively to $N_{\alpha 0}(1 - P_\alpha(E))$ and $N_\alpha(E) = N_{\alpha 0} \cdot P_\alpha(E)$.

The differential energy spectrum of the alpha particles escaping from the kernel surface for a unit of time at a solid angle of 4π is connected with $P_\alpha(E)$ through the relation (Fig. 5)

$$f_\alpha(E) = N_{\alpha 0}\frac{dP_\alpha(E)}{dE} = N_{\alpha 0}\frac{3}{4}\frac{1}{\varepsilon_\alpha(E)R}, \quad (3)$$

where $\lambda_\alpha(E) = \int dE/(-dE/dx)$ is the alpha particle path in the kernel; and $\varepsilon_\alpha(E) = (-dE/dx)$ is the stopping power of the alpha particles.

The path $1/\lambda_\alpha(E) = \Sigma(w_i/\lambda_{\alpha i})$ and the stopping power $\varepsilon_\alpha(E) = \Sigma(w_i \cdot \varepsilon_{\alpha i})$ in the kernel material and in the coating were calculated using the Bragg-Kleeman additivity rule. The path $R_{\alpha i}(E)$ and the stopping power $\varepsilon_{\alpha i}(E)$ of the i-th nuclide were calculated using the SRIM code.

Fig. 5 presents spectra of alpha particles for irradiated and unirradiated fuel. The intensity of the alpha particle generation $N_{\alpha 0}$ in the kernel in an unirradiated fuel pellet (ω_{fuel} = 17 %) is equal to ~$2.39 \cdot 10^5$ α/s/kernel; 99.9% of the alpha particles result from the decay of the ^{239,240}Pu isotopes; the average energy of the alpha particle spectrum is $\langle E_\alpha \rangle = \Sigma\delta_i \cdot E_i$ = 5.15 MeV; and the probability of the alpha particle escape from the kernel surface is $P_\alpha(5.15)$ = 7.11%.

For an irradiated fuel pellet, $N_{\alpha 0} = 3.08 \cdot 10^7$ α/s/kernel; 99.06 % of the alpha particles result from the decay of the ^{242,244}Cm isotopes; $\langle E_\alpha \rangle$ = 5.93 MeV; and $P_\alpha(5.93)$ = 7.94%. The calculation has shown that the alpha particles formed in unirradiated and irradiated fuel pellet kernels (see Fig. 5) remain in the first coating since their path lengths do not exceed 35 μm. For further calculations, the continuous spectrum $f_\alpha(E)$ was transformed into a group form for the SOURCES.

Intensity and energy spectrum of the radiation source

The subject of the study is a hexagonal fuel block of the HGTRU reactor plant (Shamanin et al. 2015, Shamanin et al. 2016, Shamanin et al. 2018) representing a block of dense high-quality graphite machined at a temperature of 3000 to 3300 K and having 76 small-diameter channels for fuel pellets of the type 1017 (∅10.17×10^{-3} m) and seven large-diameter channels (∅24×10^{-3} m) for the coolant. The flat-to-flat dimension of the fuel block is 0.207 m and its height is 0.80 m.

Fig. 6 presents the results of the neutron source calculations in terms of one fuel channel (basis) the diameter of which is 10.17×10^{-3} m and the height is 0.8 m. The fuel channel is filled with pellets of the type 1017.

The integral yield of neutrons $q_{\Sigma} = (q_{\alpha n}(^{17,18}O,^{13}C) + q_{sf})$ for ω_{fuel} = 17 % (Fig. 6, line 1) is equal to ~$4.58\cdot10^{3}$ neutr./s/basis. The contribution of neutrons from the (α, n) reactions on $^{17,18}O$ of the oxide fuel ceramics is $q_{\alpha-n}(^{17,18}O)/q_{\Sigma}$ = 41.1% (Fig. 6, line 3); the contribution of neutrons from the (α,n) reactions on ^{13}C is $q_{\alpha n}(^{13}C)/q_{\Sigma}$ = 1.18% (Fig. 6, line 4); $q_{\alpha n}(^{17,18}O,^{13}C)/q_{sf}$ = 0.7325, and $q_{\alpha n}(^{17,18}O,^{13}C) = 2.98\cdot10^{1}$ neutr./s/cm^3. For a homogeneous fuel pellet of a VVER-1000 reactor (fresh UO_2 with an enrichment of 4.4%), the similar ratio is equal to $q_{\alpha n}(^{17,18}O)/q_{sf}$ = 0.0084, and the yield is $q_{\alpha n}(^{17,18}O) = 1.011\cdot10^{-3}$ neutr./s/cm^3.

The yield of neutrons $q_{\alpha n}$ from the (α, n) reactions (see Fig. 6, line 3) for an unirradiated pellet defines the shape of the total distribution of $S_{\alpha n}(E)$ (see Fig. 6, line 1), which has the maximum in the energy region of 2.25 to 2.5 MeV. The maximum is defined by the (α, n) reaction on the $^{18,17}O$ nuclei of the oxide fuel ceramics during the interaction of the alpha particles resulting from the decay of the $^{239,240,241}Pu$ and ^{232}Th isotopes. For a homogeneous pellet, $q_{\alpha n}$ also defines the shape of $S_{\alpha n}(E)$. To describe $S_{\alpha n}(E)$, heterogeneous and homogeneous problems can use the function of the form $\chi_{\alpha n}(E) = [a(2\pi)^{1/2}]^{-1}\cdot\exp[-(E-b)^2/2a^2]$. For an irradiated heterogeneous pellet, the total yield of neutrons can be approximated by the spectral Watt function $\chi_{sf}(E) = c\times\exp(-E/a)\times\sinh(bE)^{1/2}$, since $q_{\alpha n}/q_{sf}$ = 0.0050 and $q_{\alpha n} = 8.26\cdot10^{1}$ neutr./s/cm^3 (ω_{fuel} = 17 %, Z = 400 GW·day/tTh-Pu).

The spectrum of the source of photons resulting from the decay of the $^{239,240,241}Pu$ and ^{232}Th isotopes was prepared in the Origen-Arp code in a group form and is presented in Fig. 7.

The integral yield of photons for ω_{fuel} = 17 % is equal to ~$8.2\cdot10^{10}$ gamma-quantum/s/basis. Over 99.01 % of photons are formed in the energy region of 10 to 30 keV. The energy spectra of the radiation sources (see Figs. 6, 7) were prepared in a group form for further calculations using the MCNPX2.6.0 code.

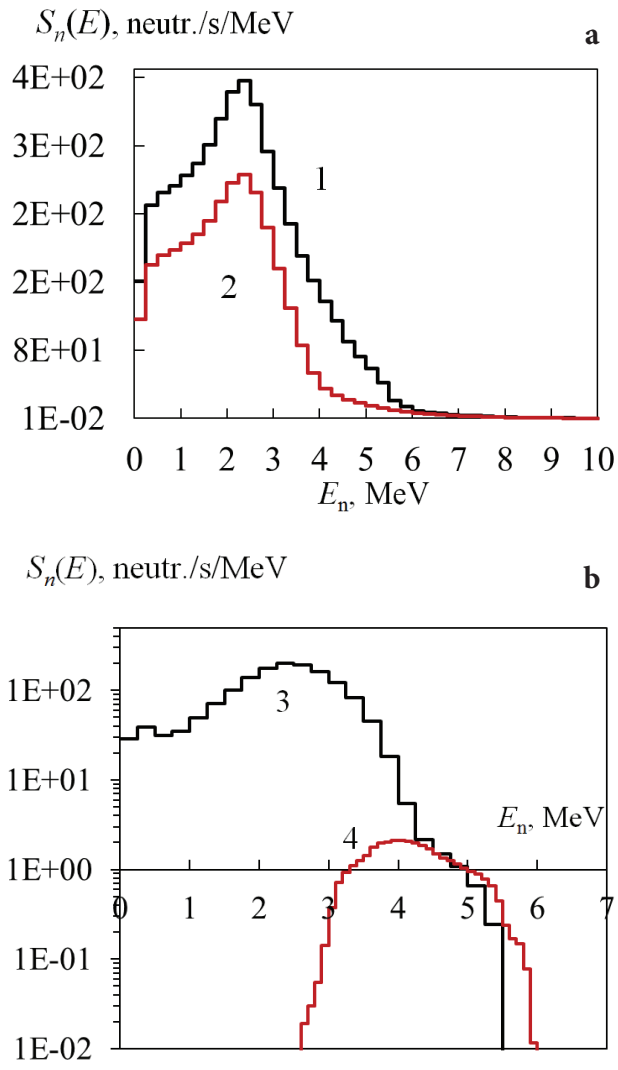

Figure 6. Energy spectrum of the neutron source: 1 – integral yield of neutrons; 2 – yield of neutrons from spontaneous fission and the (α, n) reaction on $^{17,18}O$ [$(Th,Pu)O_2$]; 3 – yield of neutrons from to the (α, n) reaction on $^{17,18}O$; 4 – yield of neutrons from the (α, n) reaction on^{13}C (RuS).

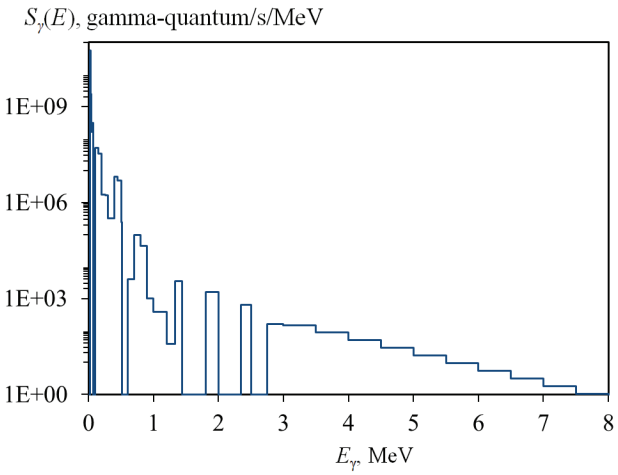

Figure 7. Energy spectrum of the photon source.

Conclusion

The fuel block investigated in this paper is a subcritical multiplying system with a complex inner structure. The (α,n) reaction in the fuel block of such reactor needs to be considered not only on the oxygen nuclei of the (Th,Pu) O_2 composition but also on the carbon nuclei contained in the first coating of dispersed microencapsulated fuel. Procedures have been developed to calculate the quantitative and spectral compositions of the neutron radiation from this fuel which made it possible to determine the ratio of the quantity of the neutrons $q_{\alpha n}$ from the (α, n) reactions to the similar quantity q_{sf} from spontaneous fission.

The tools developed as part of the study will make it possible to estimate the neutron radiation dose from the fuel under investigation, to revise the traditional procedures for handling fresh and irradiated fuel, and to estimate the neutron multiplication factor in the HGTRU fuel block using the Rossi alpha method.

The work has been supported by the Russian Scientific Fund. Grant No. 18-19-00136, dated 18.04.2018.

References

- Bak MA, Petrzhak KA, Romanov YuF (1965) Radiation of a spherical source in the presence of self-absorption. Zhurnal tekhnicheskoy fiziki, 26(2): 379–384. [in Russian]
- Bedenko S, Shamanin I, Grachev V, Knyshev V, Ukrainets O, Zorkin A (2018) Neutron radiation characteristics of the IV-th generation reactor spent fuel. AIP Conference Proceedings, 1938(020001).
- Bogatov SA, Mitenkova EF, Novikov NV (2015) The radiation characteristics of the transport packages with vitrified high-level waste. Physics of Atomic Nuclei, 78(11): 1301–1308. https://doi.org/10.1134/S106377881511006X
- Bulanenko VI (1979) Neutron yield of the (a,n) reaction on oxygen. Atomnaya energiya, 47(1): 531–534. https://doi.org/10.1007/BF01133430 [In Russian]
- Chukbar BK (2015) Verification of statistical method CORN for modeling of microfuel in the case of high grain concentration. Physics of Atomic Nuclei, 78(11): 1200–1205. https://doi.org/10.1134/S1063778815110071
- Dulin VV, Matveyenko IP (2002) Determination of deeply subcritical states of multiplying media by Rossi alpha method. Izvestiya vysshykh uchebnykh zavedeniy. Yadernaya energetika, 1: 9–18. [In Russian]
- Dulin VV, Zabrodskaya SA (2005) On the contribution of the (a, n)-reaction to the intensity of the neutron radiation of plutonium dioxide. Izvestiya vysshykh uchebnykh zavedeniy. Yadernaya energetika, 4: 18–24. [In Russian]
- Fomushkin EF (2010) Selected characteristics of the radiation distribution in spherically active systems. VANT. Ser. Fizika yadernykh reaktorov, 2010(2):17–21. [In Russian]
- Glukhov LY, Kotkov SP, Kuznetsov MS, Chursin SS (2016) Measurement of prompt neutron generation time at the VIR-2M pulsed nuclear reactor. Physics of Atomic Nuclei, 79(8): 1357–1361. https://doi.org/10.1134/S106377881608007X
- Jacobs GJH, Liskien H (1983) Energy Spectra of Neutrons Produced by a-Particles in Thick Targets of Light Elements. Annals of Nuclear Energy, 1983 (10): 541–552. https://doi.org/10.1016/0306-4549(83)90003-8
- Leniau B, Wilson JN (2014) A new spent fuel source characterization code CHARS and its application to the shielding of the thorium. Progress in Nuclear Science and Technology, 4: 134–137. https://doi.org/10.15669/pnst.4.134
- Murata T, Shibata K (2002) Evaluation of The (a, n)-reaction Nuclear Data for Light Nuclei. Journal of Nuclear Science and Technology, 39: 76–79. https://doi.org/10.1080/00223131.2002.10875044
- Shamanin IV, Bedenko SV, Chertkov YuB (2016) A small thorium reactor plant operating with a super-long life. Izvestiya vuzov. Yadernaya energetika, 2: 121–132. [In Russian]
- Shamanin IV, Bedenko SV, Chertkov YuB, Gubaydulin IM (2015) Gas-cooled nuclear reactor with thorium fuel block of a unified design. Izvestiya vysshykh uchebnykh zavedeniy. Yadernaya energetika, 3: 124–134. [In Russian]
- Shamanin IV, Bedenko SV, Nesterov VN, Lutsik IO, Prets AA (2017) Solving a system of neutron-transport multi-group equations in subcritical systems. Izvestiya vuzov. Yadernaya energetika, 4: 38–49. [In Russian]
- Shamanin IV, Grachev VM, Chertkov YuB, Bedenko SV, Mendoza O, Knyshev VV (2018) Neutronic properties of high-temperature gas-cooled reactors with thorium fuel. Annals of Nuclear Energy, 113: 286–293. https://doi.org/10.1016/j.anucene.2017.11.045
- Spirin YeV, Aleksakhin RM, Vlaskin GN, Utkin SS (2015) Radiation balance of spent nuclear fuel of a fast reactor and natural uranium. Atomnaya energiya, 119(2): 142–148. https://doi.org/10.1007/s10512-015-0040-4 [In Russian]
- Vlaskin G, Khomyakov Y (2017) Calculation of Neutron Production Rates and Spectra from Compounds of Actinides and Light Elements. EPJ Web of Conferences, 153(07033). https://doi.org/10.1051/epjconf/201715307033
- Vlaskin GN, Khomyakov YuS, Bulanenko VI (2015) Neutron yield of the (a, n) reaction on thick light-element targets. Atomnaya energiya, 117(5): 357–365. https://doi.org/10.1007/s10512-015-9933-5 [In Russian]
- West D, Sherwood AC (1982) Measurements of Thick-Target (a, n) Yields from Light Elements. Annals of Nuclear Energy, 9: 551–577. https://doi.org/10.1016/0306-4549(82)90001-9
- Wilson WB, Perry RT, Charlton WS, Parish TA (2009) Sources: A code for calculating (alpha, n) spontaneous fission, and delayed neutron sources and spectra. Progress in Nuclear Energy, 51(4–5): 608–613. https://doi.org/10.1016/j.pnucene.2008.11.007
- Ziegler JF, Ziegler MD, Biersack JP (2010) SRIM – The Stopping and Ranges of Ions in Matter. Nuclear Instruments and Methods in Physics Research B, 2010(268): 1818–1823. https://doi.org/10.1016/j.nimb.2010.02.091